

ON THE x_F DISTRIBUTION OF J/ψ 'S PRODUCED IN HEAVY ION COLLISIONS

F.O. Durães, F.S. Navarra and M. Nielsen

*Instituto de Física, Universidade de São Paulo,
C.P. 66318, 05389-970 São Paulo, SP, Brazil*

Abstract

Thermal production of J/ψ within quark gluon plasma is reconsidered. We show that if screening effects are not strong enough, the “in-plasma born” J/ψ 's would show up as a peak in the Feynman momentum distribution at $x_F = 0$.

I. INTRODUCTION

Over the past fifteen years charmonium suppression has been considered as one of the best signatures of quark gluon plasma (QGP) formation. Recently this belief was questioned by some works. J/ψ suppression in relativistic heavy ion collisions is based on the following simple argument, presented in the original work by Matsui and Satz [1]. Lattice simulations show that the heavy quark-antiquark potential becomes screened at high enough temperatures. As a consequence, when the range of the potential becomes smaller than the J/ψ Bohr radius the bound state can no longer be formed. On the other hand, detailed simulations [2] of a population of $c - \bar{c}$ pairs traversing the plasma suggested that, given the large number of such pairs, the recombination effect of the pairs into charmonium Coulomb bound states is non-negligible and can even lead to an enhancement of J/ψ production. This conclusion received support from the calculations of [3], where a two component model for J/ψ production was proposed.

Taking the existing calculations seriously, *it is no longer clear that an overall suppression of the number of J/ψ 's will be a signature of QGP*. A more detailed analysis is required and a more complex pattern can emerge. In particular, we might have suppression in some regions of the phase space and enhancement in others. Indeed, this is the result of the analysis presented in [4]. In this work the authors study the fate of $c - \bar{c}$ pairs produced in the early stage of heavy ion collisions, comparing the case where they have to traverse QGP with the case where they have to traverse ordinary nuclear matter. One of the merits of this paper is

to emphasize that very interesting information can be extracted from the scaled momentum (x_F) distribution of the produced J/ψ 's.

Motivated by these observations, in this work we address the J/ψ Feynman momentum distributions. In some aspects we follow refs. [3] and [4] with one important difference: we include J/ψ production *within the plasma*. This is usually neglected, first because the number of $c\bar{c}$ pairs produced in the plasma is small. In [5], for example, it was estimated to be of the order of 1% of the total number of charm quark pairs. In [6], with the inclusion of thermal parton masses this fraction was estimated to reach 20 – 30%. Moreover, and this was the main reason to neglect this contribution, screening was believed to destroy all bound states. Although well established in several lattice calculations [7], the color screening mechanism may be not so effective in real collisions. The existing lattice results are valid for an infinite mass, static, charge-anticharge pair and we know that this is not very close to the real situation, where charges are not so heavy and are moving. Recently, a calculation of the screening effect in moving charges [8] showed that, in this case the screening is not so strong. With the improvements of lattice gauge determinations [7] of the temperature-dependent quark-antiquark potential new calculations of the quarkonium spectrum in QGP were performed. In [9] it was found that at up to temperatures of the order of $1.10 T_c$ the J/ψ can survive as a bound state in the plasma. At higher temperatures the potential is too shallow to hold a bound charmonium state. In [10] it was found that even below the phase transition, at $T_d = 0.99T_c$ the charmonium is dissociated. This issue seems to be still controversial.

We shall assume that screening is not so strong and, in a narrow temperature window just above the phase transition, will allow for charmonium (Coulomb) bound states which “survive” from QGP. As it will be seen, these “survivors” tend to escape with $x_F \simeq 0$, thus giving us a new kind of QGP signal. Moreover, this peak at low x_F will fill the dip predicted in [4].

We will consider J/ψ production in nucleus-nucleus collisions by three different mechanisms: i) direct (primordial QCD parton fusion) ii) thermal (statistical coalescence at hadronization) and iii) QGP (in-plasma parton fusion). As already discussed in [3] i) and ii) are just two extreme cases. In realistic simulations, for a fixed number of $c\bar{c}$ pairs and of J/ψ 's, these last are gradually destroyed, giving origin to the “regenerated” component ii). As also shown in [3], for central collisions and for high enough energies there is a near to complete replacement of the initial by the final thermal J/ψ 's, but the total number stays approximately constant! Component iii) was never considered. Once produced the charmonium state will suffer interactions with the partons in the plasma, or with hadrons in hot and dense medium and in a later stage with comoving hadrons [11]. Given its relatively low binding energy (specially if medium effects are taken into account [12]) and its large mass (and large inertia), these interactions can either “make or break” [13] the bound state, changing the overall number of J/ψ 's, but *they do not change the x_F distribution of the survivors*.

Before performing detailed calculations one could try to guess the shape of the outcoming J/ψ 's x_F distribution in the three mechanisms mentioned above. QGP production has been studied in the past and the naive extrapolation of the spectra measured in $p - p$ and $p - A$ collisions would lead us to conclude that the J/ψ 's produced in i) should follow a distribution of the type [14]:

$$\simeq (1 - x_F)^c \quad (1)$$

where $c \simeq 5 - 6$. Thermal production follows a Bose-Einstein distribution [15], which integrated in p_T^2 gives:

$$\simeq \exp \left[-\frac{1}{T} \left(\sqrt{x_F^2 s/4 + m_{J/\psi}^2} \right) \right] \left[1 + \frac{1}{T} \sqrt{x_F^2 s/4 + m_{J/\psi}^2} \right] \quad (2)$$

where x_F and \sqrt{s} are the Feynman momentum and the c.m.s. nucleon-nucleon invariant energy. Comparing (1) with (2), we can see that the latter flattens out at low values of x_F , because of the mass $m_{J/\psi}$, forming a “plateau”. A spectrum from mechanism iii) is a little more difficult to predict. It involves the convolution of two distributions of the type (2) (for the two colliding massless partons) and therefore we expect it to be more steeply falling with x_F . As it will be seen, within certain approximations, it is given by:

$$\simeq \frac{1}{x_F} \quad (3)$$

According to [3] we expect real spectra to be a mixture of (1) and (2), with a small contribution from (3), which, because of its peaky structure, may be seen.

The text is organized in the following way: in section II we describe direct production; in sections III and IV we address production in the plasma and final thermal production respectively; in section V we present numerical results and in the last section we make some concluding remarks.

II. INITIAL J/ψ PRODUCTION IN NUCLEUS - NUCLEUS COLLISIONS

Nowadays perturbative QCD calculations of $c\bar{c}$ production can be found in textbooks. Nevertheless, we shall, in what follows, give some formulas to introduce the notation, to stress the role played by shadowing and to obtain expressions in terms of x_F , the variable of interest. Perhaps the most popular (and which enjoys considerable phenomenological success) approach to charm production is the Color Evaporation Model (CEM) [16,17,18]. We are aware of the discrepancies between different implementations of perturbative QCD in charm production [16]. Our results will certainly depend on the choice of approach. In spite of the uncertainties, we will assume that, since we are interested in the low x_F region, pQCD is enough and nonperturbative effects are small, in sharp contrast to what happens at large x_F [19].

In the CEM, charmonium is defined kinematically as a $c\bar{c}$ state with mass below the $D\bar{D}$ threshold. In leading order (LO) the cross section is computed with the use of perturbative QCD for the diagrams of the elementary processes $q\bar{q} \rightarrow c\bar{c}$ and $gg \rightarrow c\bar{c}$ convoluted with the parton densities in the projectile and in the target. Calling x_F the fractional momentum of the produced pair (with respect to the momentum of a projectile nucleon in cm frame)

and \sqrt{s} the cm energy of a nucleon-nucleon collision, the cross section for production of a $c\bar{c}$ pair with mass m is just given by:

$$\begin{aligned} \frac{d\sigma^{pp\rightarrow c\bar{c}}}{dx_F dm^2} &= \int_0^1 dx_1 dx_2 \delta(x_1 x_2 s - m^2) \delta(x_F - x_1 + x_2) H(x_1, x_2; m^2) \\ &= \frac{1}{s \sqrt{x_F^2 + 4m^2/s}} H(x_{01}, x_{02}; m^2) \quad ; \quad x_{01,02} = \frac{1}{2} \left(\pm x_F + \sqrt{x_F^2 + 4m^2/s} \right) \end{aligned} \quad (4)$$

where x_1 and x_2 are the nucleon momentum fractions carried respectively by partons in the projectile and target. The function $H(x_1, x_2; m^2)$, which represents the convolution of the elementary cross sections and parton densities is given by:

$$\begin{aligned} H(x_1, x_2; m^2) &= f_g(x_1, m^2) f_g(x_2, m^2) \hat{\sigma}_{gg}(m^2) \\ &\quad + \sum_{q=u,d,s} [f_q(x_1, m^2) f_{\bar{q}}(x_2, m^2) + f_{\bar{q}}(x_1, m^2) f_q(x_2, m^2)] \hat{\sigma}_{q\bar{q}}(m^2) \end{aligned} \quad (5)$$

with the parton densities $f_i(x, m^2)$ in the nucleon computed at the scale $m^2 = x_1 x_2 s$.

The LO elementary cross sections in terms of the pair invariant mass (m) are given by [20]:

$$\hat{\sigma}_{gg}(m^2) = \frac{\pi \alpha_s^2(m^2)}{3m^2} \left\{ \left(1 + \frac{4m_c^2}{m^2} + \frac{m_c^4}{m^4} \right) \ln \left[\frac{1+\lambda}{1-\lambda} \right] - \frac{1}{4} \left(7 + \frac{31m_c^2}{m^2} \right) \lambda \right\} \quad (6)$$

$$\hat{\sigma}_{q\bar{q}}(m^2) = \frac{8\pi \alpha_s^2(m^2)}{27m^2} \left(1 + \frac{2m_c^2}{m^2} \right) \lambda \quad ; \quad \lambda = \left[1 - \frac{4m_c^2}{m^2} \right]^{1/2} \quad (7)$$

where m_c is the mass of the c quark.

The production cross section of the charmed state i ($= J/\psi, \psi'$ or χ_{cJ}) σ_i , is then finally obtained by integrating the free pair cross section $c\bar{c}$ over the invariant mass m starting from the production threshold $2m_c$ up to open charm production threshold $2m_D$:

$$\frac{d\sigma^{pp\rightarrow J/\psi X}}{dx_F} = F_{J/\psi} \int_{4m_c^2}^{4m_D^2} dm^2 \frac{d\sigma^{pp\rightarrow c\bar{c}}}{dx_F dm^2} \quad (8)$$

where $F_{J/\psi}$ is the fraction of $\sigma^{c\bar{c}}$ which contains the corresponding $c\bar{c}$ resonance.

This model describes well the experimentally measured x_F distribution of hidden charm both with LO and NLO cross sections, provided that F_i^{LO} is defined as F_i^{NLO} multiplied by a theoretical factor κ , which is equal to the ratio of the NLO and LO cross sections ($F_{J/\psi}^{NLO} \approx 2, 54\%$) [21].

In what follows we shall use the CEM to study perturbative J/ψ production in nucleus-nucleus collisions at RHIC. As it is well known, in nuclear collisions and in processes involving small values of x , shadowing plays an important role (see, for example, [22]). In this case expression (5) is rewritten as:

$$\begin{aligned} H_{AB}(x_1, x_2; m^2) &= A B \left\{ f_g(x_1, m^2) R_g^A(x_1, m^2) f_g(x_2, m^2) R_g^B(x_2, m^2) \hat{\sigma}_{gg}(m^2) \right. \\ &\quad + \sum_{q=u,d,s} \left[f_q(x_1, m^2) R_q^A(x_1, m^2) f_{\bar{q}}(x_2, m^2) R_{\bar{q}}^B(x_2, m^2) \right. \\ &\quad \left. \left. + f_{\bar{q}}(x_1, m^2) R_{\bar{q}}^A(x_1, m^2) f_q(x_2, m^2) R_q^B(x_2, m^2) \right] \hat{\sigma}_{q\bar{q}}(m^2) \right\} \end{aligned} \quad (9)$$

where

$$R_i^A(x, m^2) = \frac{f_i^A(x, m^2)}{f_i(x, m^2)} \quad (10)$$

with $f_i^A(x, m^2)$ being the i parton momentum distribution in a nucleon inside the nucleus A . Replacing H by H_{AB} in (4) we obtain the cross section for $c\bar{c}$ production in $A - B$ collisions, from which we obtain the J/ψ production cross section as:

$$\frac{d\sigma^{AB \rightarrow J/\psi}}{dx_F} = \kappa F_{J/\psi}^{NLO} \frac{d\sigma^{AB \rightarrow c\bar{c}}}{dx_F} = \kappa F_{J/\psi}^{NLO} \int_{4m_c^2}^{4m_D^2} dm^2 \frac{1}{s \sqrt{x_F^2 + 4m^2/s}} H_{AB}(x_{01}, x_{02}; m^2) \quad (11)$$

In a central $A + A$ collision the number of J/ψ 's produced directly is related to the cross section by [23]:

$$\frac{dN_{direct}^{AB \rightarrow J/\psi}}{dx_F} \cong \frac{1}{\pi R_A^2} \frac{d\sigma_{QCD}^{AB \rightarrow J/\psi}}{dx_F} = \frac{1}{\pi R_A^2} \kappa F_{J/\psi}^{NLO} \frac{d\sigma_{QCD}^{AA \rightarrow c\bar{c}}}{dx_F} \quad (12)$$

where R_A is the radius of nucleus A .

The expression above would give the final distribution if there were no absorption due to further interactions with partons in a QGP or hadrons in a comoving fireball. This is certainly not realistic. We know that interactions may well occur, but they will only destroy the bound state, reducing the normalization of (12) but not changing its x_F dependence.

III. J/ψ PRODUCTION IN THE PLASMA

As in the previous section we reproduce below (to a great extent) textbook material [24], with the purpose of defining our notation. The derivation presented here is also useful because, relaxing the screening hypothesis, we calculate the production of charm *bound states* in the plasma and we integrate the rate on all variables except x_F . All this requires some straightforward but not very often shown manipulations.

The computation of the in-plasma $c\bar{c}$ pair production rate goes back to the late eighties [25], was discussed in short papers (for example [5]), included in comprehensive review articles [26] during the nineties and experienced improvements due to advances in thermal field theory [6]. The in-plasma bound state production was always discarded in view of the screening.

Assuming that QGP is formed, we then have a gas of quarks and gluons with momenta obeying respectively Fermi-Dirac and Bose-Einstein distributions that can collide producing $c\bar{c}$ pairs. This is the same mechanism, which in the strange sector causes the strangeness enhancement. In the charm case, there will be always a ‘‘charm enhancement’’ but, because of screening, the charmed quarks will mostly form open charm. In the present calculation we will let part of the thermally produced charm Coulomb bound states escape. Since the temperature is high, there will be a significant number of parton-parton collisions at a cms energy high enough to produce charm quark pairs, which will form charmonium states. We will now estimate their production rate using the CEM in a thermal environment.

The charmonium production rate in the reaction $gg \rightarrow c\bar{c}$, at temperature T is given by [24]:

$$\frac{dN^{gg \rightarrow c\bar{c}}}{dt d^3x} = \frac{1}{(2\pi)^6} g_{gg}^2 \int d^3p_1 d^3p_2 f_g(E_1) f_g(E_2) \hat{\sigma}_{gg}^{LO}(m^2) v_{12} \quad (13)$$

where g_g is the gluon statistical factor (number of colors \times number polarization states) v_{12} is the relative velocity between colliding gluons with energies E_1 and E_2 and three momenta \vec{p}_1 and \vec{p}_2 , $\hat{\sigma}_{gg}$ is the elementary gluon-gluon cross section (6) and $f_g(E_i)$ the usual thermal distribution function:

$$f_g(E_i) = \frac{1}{e^{E_i/T} - 1} \quad (14)$$

We now introduce the charm pair four momentum p with help of the delta function $\delta^4[p - (p_1 + p_2)]$:

$$\frac{dN^{gg \rightarrow c\bar{c}}}{d^4p} = \frac{1}{(2\pi)^6} g_{gg}^2 \int dt d^3x d^3p_1 d^3p_2 f_g(E_1) f_g(E_2) \hat{\sigma}_{gg}^{LO}(m^2) v_{12} \delta^4[p - (p_1 + p_2)] \quad (15)$$

In the expression above we have:

$$p_1 \equiv (E_1, \vec{p}_{T_1}, p_{z_1}) \quad ; \quad p_2 \equiv (E_2, \vec{p}_{T_2}, p_{z_2}) \quad ; \quad p \equiv (E, \vec{p}_T, p_z) \quad (16)$$

$$m^2 = (p_1 + p_2)^2 \quad ; \quad v_{12} = \frac{1}{2} \frac{m^2}{E_1 E_2} \quad (17)$$

where m is the invariant mass of the pair. We next decompose the delta function into temporal, transverse and longitudinal components:

$$\begin{aligned} \frac{dN^{gg \rightarrow c\bar{c}}}{dm^2 d\vec{p}_T dp_z} &= \frac{1}{2(2\pi)^6} g_{gg}^2 \int dt d^3x \frac{1}{E_1} d^3p_1 \frac{1}{E_2} d^3p_2 f_g(E_1) f_g(E_2) \hat{\sigma}_{gg}^{LO}(m^2) m^2 \\ &\quad \times \delta[m^2 - (p_1 + p_2)^2] \delta^2[\vec{p}_T - (\vec{p}_{T_1} + \vec{p}_{T_2})] \delta[p_z - (p_{z_1} + p_{z_2})] \end{aligned} \quad (18)$$

Making use of the identity

$$\int \frac{1}{2E_i} d^3p_i = \int d^4p_i \delta(p_i^2) \theta(E_i) = \int dE_i d\vec{p}_{T_i} dp_{z_i} \delta[E_i^2 - p_{T_i}^2 - p_{z_i}^2] \theta(E_i) \quad (19)$$

we arrive at:

$$\begin{aligned} \frac{dN^{gg \rightarrow c\bar{c}}}{dm^2 d\vec{p}_T dp_z} &= \frac{2}{(2\pi)^6} g_{gg}^2 \int dt d^3x \int_0^\infty dE_1 \int_{-\infty}^\infty d\vec{p}_{T_1} \int_{-\infty}^\infty dp_{z_1} \delta[E_1^2 - p_{T_1}^2 - p_{z_1}^2] \theta(E_1) \\ &\quad \times \int_0^\infty dE_2 \int_{-\infty}^\infty d\vec{p}_{T_2} \int_{-\infty}^\infty dp_{z_2} \delta[E_2^2 - p_{T_2}^2 - p_{z_2}^2] \theta(E_2) f_g(E_1) f_g(E_2) \\ &\quad \times \hat{\sigma}_{gg}^{LO}(m^2) m^2 \delta[m^2 - (p_1 + p_2)^2] \delta^2[\vec{p}_T - (\vec{p}_{T_1} + \vec{p}_{T_2})] \delta[p_z - (p_{z_1} + p_{z_2})] \end{aligned} \quad (20)$$

Integrating in p_{z_2} , p_{T_1} , p_{T_2} and E_2 and defining β as the angle between \vec{p}_T and \vec{p}_{T_1} , we finally obtain:

$$\begin{aligned}
\frac{dN^{gg \rightarrow J/\psi}}{dp_z} &= \frac{\pi}{2(2\pi)^6} g_{gg}^2 \int_{4m_c^2}^{4m_D^2} dm^2 \int_0^\infty dp_T^2 \int_0^{2\pi} d\beta \int dt d^3x \int_0^\infty dE_1 \int_{-\infty}^\infty dp_{z_1} f_g(E_1) f_g(E - E_1) \\
&\times \hat{\sigma}_{gg}^{LO}(m^2) \frac{m^2}{E} \delta[m^2 - 2EE_1 + 2p_T(E_1^2 - p_{z_1}^2)^{1/2} \cos(\beta) + 2p_z p_{z_1}] \\
&\times \theta(E_1) \theta(E - E_1) \theta(E_1^2 - p_{z_1}^2) \\
&= \frac{\pi}{2(2\pi)^6} g_{gg}^2 \int_{4m_c^2}^{4m_D^2} dm^2 \int_0^\infty dp_T^2 \int_0^{2\pi} d\beta \int dt d^3x \int_0^\infty dE_1 f_g(E_1) f_g(E - E_1) \\
&\times \hat{\sigma}_{gg}^{LO}(m^2) \frac{m^2}{E} \left[\frac{1}{|H(h_1)|} \theta(E_1^2 - h_1^2) + \frac{1}{|H(h_2)|} \theta(E_1^2 - h_2^2) \right] \theta(E_1) \theta(E - E_1) \quad (21)
\end{aligned}$$

where E , $H(h_{1,2})$ and $h_{1,2}$ are given by:

$$E = [m^2 + p_T^2 + p_z^2]^{1/2} ; \quad H(h_{1,2}) = 2p_z - \frac{2p_T \cos(\beta)}{(E_1^2 - h_{1,2}^2)^{1/2}} h_{1,2} \quad (22)$$

$$\begin{aligned}
h_{1,2} &= \frac{1}{2} \frac{1}{p_z^2 + p_T^2 \cos^2(\beta)} \left\{ p_z (2EE_1 - m^2) \mp \{ p_T^2 \cos^2(\beta) \right. \\
&\times [4E_1^2 (p_T^2 \cos^2(\beta) + p_z^2) - (m^2 - 2EE_1)^2] \}^{1/2} \left. \right\} \quad (23)
\end{aligned}$$

In the first line of (21) we have $\delta[m^2 - 2EE_1 + 2p_T(E_1^2 - p_{z_1}^2)^{1/2} \cos(\beta) + 2p_z p_{z_1}]$. It is easy to see that taking either $E_1 \simeq p_{z_1}$ or $E_1 \gg p_{z_1}$ and using the δ function to perform the integral in p_{z_1} we obtain a factor $1/p_z$. This factor survives and, at the end, gives the $1/x_F$ structure (3) mentioned in the introduction. The actual numerical calculation involves no approximation and has a similar behavior. Notice that, because of the kinematical cuts in the invariant mass integral, we are now restricting the result to the rate to charmonium states. A similar expression can be derived for $c\bar{c}$ production originating from quark-antiquark annihilation:

$$\begin{aligned}
\frac{dN^{q\bar{q} \rightarrow J/\psi}}{dp_z} &= \frac{\pi}{2(2\pi)^6} g_{q\bar{q}}^2 \sum_{q=u,d,s} \int_{4m_c^2}^{4m_D^2} dm^2 \int_0^\infty dp_T^2 \int_0^{2\pi} d\beta \int dt d^3x \int_0^\infty dE_1 f_q(E_1) f_{\bar{q}}(E - E_1) \\
&\times \hat{\sigma}_{q\bar{q}}^{LO}(m^2) \frac{m^2}{E} \left[\frac{1}{|H(h_1)|} \theta(E_1^2 - h_1^2) + \frac{1}{|H(h_2)|} \theta(E_1^2 - h_2^2) \right] \theta(E_1) \theta(E - E_1) \quad (24)
\end{aligned}$$

where $g_{q(\bar{q})}$ is the statistical factor for quarks (antiquarks) (number of colors \times number of spin states), $\hat{\sigma}_{q\bar{q}}^{LO}(m^2)$ is given by (7) and $f_{q,\bar{q}}(E_i)$ is the usual quark thermal distribution function:

$$f_{q,\bar{q}}(E_i) = \frac{1}{e^{E_i/T} + 1} \quad (25)$$

In order to account for expansion effects we shall assume that the system cools down following Bjorken hydrodynamics, in which temperature and proper time are related by [24]:

$$\frac{T(\tau)}{T_0} = \left(\frac{\tau_0}{\tau} \right)^{1/3} \quad (26)$$

where T_0 is the initial temperature and τ_0 is the thermalization time, which marks the beginning of the hydrodynamical expansion. With the help of this relation we can perform the following change of variables:

$$dt d^3x = dx_{\perp} \tau dy d\tau = -3 dV \tau_0 T_0^3 T^{-4} dT \implies \int dt d^3x = 3 \int_{T_f}^{T_0} \tau_0 T_0^3 T^{-4} V(T) dT \quad (27)$$

Finally we introduce the energy scale \sqrt{s} (the invariant energy of a single nucleon-nucleon collision):

$$p_z = x_F \frac{\sqrt{s}}{2} \quad (28)$$

Expressions (21) and (24) can thus be rewritten as:

$$\begin{aligned} \frac{dN^{gg \rightarrow J/\psi}}{dx_F} &= \frac{3\pi}{4(2\pi)^6} g_{gg}^2 \sqrt{s} \int_{4m_c^2}^{4m_D^2} dm^2 \int_0^{\infty} dp_T^2 \int_0^{2\pi} d\beta \int_{T_f}^{T_0} \tau_0 T_0^3 T^{-4} V(T) dT \int_0^{\infty} dE_1 \\ &\times f_g(E_1) f_g(E - E_1) \hat{\sigma}_{gg}^{LO}(m^2) \frac{m^2}{E} \left[\frac{1}{|H(h_1)|} \theta(E_1^2 - h_1^2) + \frac{1}{|H(h_2)|} \theta(E_1^2 - h_2^2) \right] \\ &\times \theta(E_1) \theta(E - E_1) \end{aligned} \quad (29)$$

$$\begin{aligned} \frac{dN^{q\bar{q} \rightarrow J/\psi}}{dx_F} &= \frac{3\pi}{4(2\pi)^6} g_{q\bar{q}}^2 \sqrt{s} \sum_{q=u,d,s} \int_{4m_c^2}^{4m_D^2} dm^2 \int_0^{\infty} dp_T^2 \int_0^{2\pi} d\beta \int_{T_f}^{T_0} \tau_0 T_0^3 T^{-4} V(T) dT \int_0^{\infty} dE_1 \\ &\times f_q(E_1) f_{\bar{q}}(E - E_1) \hat{\sigma}_{q\bar{q}}^{LO}(m^2) \frac{m^2}{E} \left[\frac{1}{|H(h_1)|} \theta(E_1^2 - h_1^2) + \frac{1}{|H(h_2)|} \theta(E_1^2 - h_2^2) \right] \\ &\times \theta(E_1) \theta(E - E_1) \end{aligned} \quad (30)$$

The volume of the system evolves in time according to:

$$V(\tau) = V_0 \frac{\tau}{\tau_0} \implies V(T) = V_0 \left(\frac{T_0}{T} \right)^3 \quad (31)$$

where $V_0 = \pi R_A^2 \tau_0$, $R_A = (1.18 A^{1/3} - 0.45) (fm)$.

With all these definitions we can now evaluate the differential yield of J/ψ formed in (and “escaping” from) the quark-gluon plasma as the sum of expressions (29) and (30):

$$\frac{dN_{QGP}^{AA \rightarrow J/\psi}}{dx_F} = f_s \left[\frac{dN^{gg \rightarrow J/\psi}}{dx_F} + \frac{dN^{q\bar{q} \rightarrow J/\psi}}{dx_F} \right] \quad (32)$$

The “screening factor” f_s is the only free number introduced here. It gives the probability that a J/ψ formed inside the plasma survives the passage through the medium. In other words, f_s accounts for dynamical screening, in which gluons in the plasma destroy the charmonium bound state. It varies from 0 to 1. A literal interpretation of [1] or [7] would imply $f_s = 0$. We will however tolerate a small value of f_s and examine the consequences.

IV. FINAL THERMAL J/ψ PRODUCTION

We will also, for completeness, consider the case where the J/ψ 's produced in the early stage of the collision traverse the plasma being destroyed and then “regenerated” [3]. We call them “thermal”. As has been discussed in the literature [15,27], regenerated J/ψ 's follow a thermal distribution with the temperature of the quark-hadron phase transition $T_c \simeq 170$ MeV:

$$\begin{aligned} \frac{dN_{thermal}^{AA \rightarrow J/\psi}}{dx_F} &= \frac{\pi\sqrt{s}V_0A}{2} \int_0^s dp_T^2 \exp \left[-\frac{1}{T_c} (x_F^2 s/4 + p_T^2 + m_{J/\psi}^2)^{1/2} \right] \\ &= \text{const} \exp \left[-\frac{1}{T_c} \left(\sqrt{x_F^2 s/4 + m_{J/\psi}^2} \right) \right] \left[1 + \frac{1}{T_c} \sqrt{x_F^2 s/4 + m_{J/\psi}^2} \right] \end{aligned} \quad (33)$$

where the constant in front of the integral are not relevant since we will normalize $N_{thermal}^{AA \rightarrow J/\psi}$ to the number of initially produced charmonium states.

V. NUMERICAL RESULTS AND DISCUSSION

In Fig. 1 we show, for $Au - Au$ ($\sqrt{s} = 200$ GeV) (1a) and $Pb - Pb$ ($\sqrt{s} = 17$ GeV) (1b) collisions, the results obtained with (12) (dotted line), (32) (solid line) and (33) (dashed line). In each figure all curves are normalized to the same number of produced J/ψ 's, which is given by the integral of (12) over x_F . Using the parton distributions of [28] we obtain $N_{J/\psi} \simeq 0.09$ at RHIC and $N_{J/\psi} \simeq 0.001$ at SPS. These numbers are very close to those obtained in Ref. [29].

Although the normalization is still artificial (it overestimates the number of J/ψ 's produced in QGP) it anticipates our main claim: QGP production will create a peak at $x_F \simeq 0$. Even if suppressed, it will leave a signal. Moreover, this may happen at RHIC, as it can be seen in Fig. 1a, but did not happen at SPS, as we see in Fig. 1b, where QGP production is covered by thermal production. For the QCD distribution, we have used the nuclear parton distribution functions (PDF) parametrized as in [28]. In doing so, the proton PDF were taken from [30] (GRV98 LO). We also used $m_c = 1.2$ GeV, $m_D = 1.87$ GeV and $\kappa = 2$. With these choices the total number of produced J/ψ 's is determined. This condition fixes also the normalization of (33). We used here $T_c = 170$ MeV. In computing (32) we have used $\tau_0 = 0.7$ fm and $T_0 = 550$ MeV, for $Au + Au$ and $\tau_0 = 1$ fm and $T_0 = 300$ MeV for $Pb + Pb$ collisions. We can clearly observe that in SPS conditions the plasma production is difficult to be seen. In the case of RHIC collisions, the situation seems more promising.

In order to further investigate the differences between the three J/ψ production mechanisms we will study the relation between the measured number of J/ψ 's and the naive expectation based on what we know from pp collisions. Experimentally this ratio is easily constructed from the measured x_F spectra in $A + A$ and $p + p$ collisions. Theoretically, the numerator can be written in terms of our theoretical prejudices.

As a starting point, we assume that all J/ψ 's are produced directly and show in Fig. 2 the following ratio:

$$R_I(x_F) = \frac{\frac{1}{\pi R_A^2} \frac{d\sigma_{QCD}^{AA \rightarrow J/\psi X}}{dx_F}}{T_{AA}(b=0) \frac{d\sigma^{pp \rightarrow J/\psi X}}{dx_F}} = \frac{\frac{dN_{direct}^{AB \rightarrow J/\psi}}{dx_F}}{T_{AA}(b=0) \frac{d\sigma^{pp \rightarrow J/\psi X}}{dx_F}} \quad (34)$$

where the denominator is given by the product of (8) with the nuclear overlap function $T_{AA}(b=0) = 29.3 \text{ mb}^{-1}$ at RHIC and $= 30.4 \text{ mb}^{-1}$ at SPS. The numerators were obtained with (11), (12) and the nuclear parton distribution functions (PDF) parametrized as in [28] (solid line) and as in [31] (dashed line). In the first case the proton PDF were taken from [30] (GRV98 LO) whereas in the second case they were taken from [32] (MRST LO). With this last set of parton distributions $N_{J/\psi} \simeq 0.06$ at RHIC and $N_{J/\psi} \simeq 0.001$ at SPS.

R_I shows essentially the effect of shadowing in the low x region. We can see that if no effect is present, other than shadowing, J/ψ spectrum produced in AA collisions is just a constant times the corresponding pp spectrum. As it can be seen this constant may change a lot with the PDF. This constancy in the region $x_F < 0.1$ will be important for the subsequent discussion. This figure shows also that the value of the constant decreases when we go from SPS to RHIC collisions. This same behavior was found in [4].

If we believe that all production is mainly direct plus some small plasma component, then (34) acquires the form:

$$R_{II}(x_F) = \frac{\frac{dN_{direct}^{AA \rightarrow J/\psi X}}{dx_F} + f_s \frac{dN_{QGP}^{AA \rightarrow J/\psi X}}{dx_F}}{T_{AA}(b=0) \frac{d\sigma^{pp \rightarrow J/\psi X}}{dx_F}} \quad (35)$$

If the screening in the plasma is so strong that $f_s = 0$, then, $R_{II} = R_I \simeq const.$ If, however, there is a small J/ψ survival probability, for example $f_s = 10^{-5}$, there will be a noticeable change in R_{II} . This is illustrated in Fig. 3, where we see a pronounced deviation from a flat behavior in the low x_F region if there is a contribution from the plasma. This interesting feature is due to nature of plasma production, which is peaked at $x_F \simeq 0$. In all cases solid and dashed lines mean the same PDF's as before. We can clearly see that deviations from unity happen more strongly for RHIC collisions. Figs. 3a) and 3b) refer to $Au + Au$ at RHIC, whereas Figs. 3c) and 3d) to $Pb + Pb$ at SPS. In the figures on the left side (3a and 3c) we just use our input parameters as in the previous figures. In the figures on the right side (3b and 3d) we have normalized the direct production to a larger value of $N_{direct}^{AA \rightarrow J/\psi X}$, in such a way that it corresponds to $N_{direct}^{AA \rightarrow c\bar{c}X} = 8$ (at RHIC) and $= 0.15$ (at SPS). We did this because there are uncertainties in the QCD calculations found in the literature and these last numbers are often quoted. Different choices for the total number of $c\bar{c}$ pairs change our curves but do not change our conclusions.

The above situation has to be regarded as an extreme case, in which J/ψ 's are produced via parton fusion (with shadowing taken into account) in the initial state of the nucleus-nucleus collision and then just escape from the fireball, without further nuclear or comover suppression. We now consider the opposite extreme case, where all J/ψ 's are formed in the final state. Final state here means that the original J/ψ 's are totally destroyed by plasma screening and recreated at the final stage of the fireball life (at $T = T_c \simeq 170 \text{ MeV}$) by coalescence and then just "emerge ready" during the phase transition, having no further interaction and obeying the thermal distribution (33). This scenario is supported by the

calculations performed in [3]. Assuming this production mechanism the ratio defined above is modified to:

$$R_{III}(x_F) = \frac{\frac{dN_{Thermal}^{AA \rightarrow J/\psi X}}{dx_F} + f_s \frac{dN_{QGP}^{AA \rightarrow J/\psi X}}{dx_F}}{T_{AA}(b=0) \frac{d\sigma^{pp \rightarrow J/\psi X}}{dx_F}} \quad (36)$$

and plotted in Fig. 4. In Fig. 4a) we see that there is already a rise of R_{III} at decreasing values of x_F , but this rise has the shape of a plateau (as anticipated in the introduction), starting from $x_F \simeq 0.01$ (two lower curves). If the screening is less effective, $f_s = 10^{-4}$, then we find a deviation from the plateau (two upper curves). From Fig. 4b) we conclude that QGP production can hardly be detected at SPS since the x_F distribution is always dominated by the thermal (plateau-like) contribution. On the other hand, it should be remarked that if a plateau is found experimentally, this is interesting in itself, being a strong evidence in favor of the statistical hadronization model.

Now we come back to the prediction made in [4], namely that the initially produced J/ψ 's after the interaction either with hadronic comovers or with the plasma will disappear around $x_F \simeq 0$ giving place to a dip in this region. We can split Eq. (35) into two pieces, the first one containing initial production and the second containing the plasma contribution. In order to include the suppression resulting from final state interactions predicted in [4], we replace the first piece by a parametrization of $R_{AB}(x_F, b=0)$, Eq. (3) of [4], keep our plasma contribution the same and construct a new version of (34):

$$R_{IV}(x_F) = R_{AB}(x_F) + \frac{f_s \frac{dN_{QGP}^{AA \rightarrow J/\psi X}}{dx_F}}{T_{AA}(b=0) \frac{d\sigma^{pp \rightarrow J/\psi X}}{dx_F}} \quad (37)$$

This quantity is plotted in Fig. 5. We can observe that the plasma contribution not only fills the dip, but can generate a quite visible peak in the region $x_F < 0.01$. This peak grows rapidly from the SPS to RHIC.

VI. CONCLUSIONS

In this paper we have considered J/ψ production in nucleus-nucleus collisions by three different mechanisms: direct (primordial parton fusion) ii) thermal (statistical coalescence at hadronization) and iii) QGP (in-plasma parton fusion). As already discussed in [3] i) and ii) are just two extreme cases. In realistic simulations, for a fixed number of $c\bar{c}$ pairs and of J/ψ 's, these last are gradually destroyed, giving origin to the ‘‘regenerated’’ component ii). Component iii) is considered here for the first time. Our main point was that, even being small, contribution iii) is very strongly peaked around $x_F \simeq 0$ and can thus become visible if enough plasma is formed.

With this in mind we calculated the measurable ratio (34) and computed it assuming mechanism i) plus a small component of iii) (ratio R_{II}) and assuming mechanism ii) plus a small component of iii) (ratio R_{III}). In the first case it is completely flat without plasma contribution. A QGP contribution creates a big bump at $x_F < 0.01$. In the second case, without plasma contribution, we observe a step structure, with a plateau at $x_F < 0.01$.

Switching on the plasma contribution creates a steeply falling curve. We believe that any of these features can be measured and will be very interesting for charm physics at RHIC.

In [4] it was suggested that the x_F distribution to be measured at RHIC is flat and has a dip in the region $x_F \simeq 0$. Our calculations indicate that the inclusion of the “in-plasma born” J/ψ 's will fill this dip.

Of course, there are several improvements that one could do in the in-plasma production, as, for example, the use of a more sophisticated hydrodynamical expansion. Our findings in this work encourage us to pursue this program.

Acknowledgements: This work was partially supported by FAPESP under contract 00/04422-7. We are grateful to R. Vogt, P. Levai and X.N. Wang for useful discussions.

REFERENCES

- [1] T. Matsui and H. Satz, *Phys. Lett.* **B178**, 416 (1986); H. Satz, *Rept. Prog. Phys.* **63**, 1511 (2000).
- [2] R. L. Thews, “Nonlinear behavior of quarkonium formation and deconfinement signals”, hep-ph/0206179; R. L. Thews and J. Rafelski, *Nucl. Phys.* **A698**, 575 (2002); R. L. Thews, M. Schroedter, J. Rafelski *Phys. Rev.* **C63**, 054905 (2001).
- [3] L. Grandchamp and R. Rapp, hep-ph/0209141; *Nucl. Phys.* **A709**, 415 (2002); *Phys. Lett.* **B523**, 60 (2001).
- [4] B.Z. Kopeliovich, A. Polleri and J. Hüfner, *Phys. Rev. Lett.* **87**, 112302 (2001) and references therein.
- [5] B. Mueller and X.N. Wang, *Phys. Rev. Lett.* **68**, 2437 (1992).
- [6] R. Vogt and P. Levai, *Phys. Rev.* **C56**, 2707 (1997).
- [7] F. Karsch, *Lect. Notes Phys.* **583**, 209 (2002); *Nucl. Phys.* **A698**, 199 (2002) and references therein.
- [8] S.C. Benzahra, “Screened potential of a moving meson in a quark gluon plasma”, hep-ph/0105048; “Dissociation of a boosted quarkonium in a quark gluon plasma”, hep-ph/0204177 .
- [9] S. Digoal, P. Petreczky and H. Satz, *Phys. Rev.* **D64**, 094015 (2001).
- [10] C.Y. Wong, “Dissociation of Heavy Quarkonia in the Quark-Gluon Plasma”, nucl-th/0112064.
- [11] For recent developments in this field see F.S. Navarra, M. Nielsen and M.R. Robilotta, *Phys. Rev.* **C64**, 021901 (R) (2001); F.S. Navarra, M. Nielsen, R.S. Marques de Carvalho and G. Krein, *Phys. Lett.* **B529**, 87 (2002).
- [12] C.Y. Wong, *Phys. Rev.* **C65**, 034902 (2002).
- [13] This fine expression was coined in P. Hoyer, N. Marchal and S. Peigné, “Comover Enhancement of Quarkonium Production”, hep-ph/0209365.
- [14] See for example: A. Gribushin *et al.* (E672/E706 Collab.), *Phys. Rev.* **D62**, 012001 (2000).
- [15] P. Braun-Munzinger and J. Stachel, *Phys. Lett.* **B490**, 196 (2000); *Nucl. Phys.* **A690**, 119c (2001).
- [16] R. Vogt, *Proc. 18th Winter Workshop on Nuclear Dynamics*, 000-000 (2002), hep-ph/0203151.
- [17] R. Vogt, *Phys. Rept.* **310**, 197 (1999).
- [18] V. Barger, W. Y. Keung and R. N. Philips, *Phys. Lett.* **B91**, 253 (1980).
- [19] F. Carvalho, F.O. Durães, F.S. Navarra and M. Nielsen, *Phys. Rev. Lett.*, **86**, 5434 (2001); F.O.Durães, F.S.Navarra, C. A. A. Nunes and G.Wilk, *Phys. Rev.* **D53**, 6136 (1996) .
- [20] M. Glück and E. Reya, *Phys. Lett.* **B79**, 453 (1978).
- [21] R. V. Gavai *et al.*, *Int. J. Mod. Phys.* **A10**, 3043 (1995).
- [22] N. Hammon, L. Gerland, H. Stoecker and W. Greiner, *Phys. Rev.* **C59**, 2744 (1999).
- [23] K. J. Eskola, K. Kajantie and J. Lindfors *Nucl. Phys.* **B323**, 37 (1989).
- [24] “*Introduction to High-Energy Heavy-Ion Collisions*, Cheuk-Yin Wong, World Scientific Publishing Co. Pte. Ltd, 1994.
- [25] A. Shor, *Phys. Lett.* **B215**, 375 (1988).
- [26] J. Rafelski, J. Letessier and A. Tounsi, *Acta Phys. Pol.* **B27**, 1037 (1996).

- [27] M.I. Gorenstein, A.P. Kostyuk, H. Stoecker and W. Greiner, *Phys. Lett.* **B509**, 277 (2001); *J. Phys.* **G27**, L47 (2001).
- [28] K. J. Eskola, V. J. Kolhinen and C. A. Salgado, *Eur. Phys. J.* **C9**, 61 (1999).
- [29] R. L. Thews, *Nucl. Phys.* **A702**, 341 (2002).
- [30] M. Glück and E. Reya and A. Vogt, *Eur. Phys. J.* **C5**, 461 (1998).
- [31] M. Hirai, S. Kumano and M. Miyama, *Phys. Rev.* **D64**, 034003 (2001).
- [32] A. D. Martin *et al.*, *Eur. Phys. J.* **C4**, 463 (1998); *Phys. Lett.* **B443**, 301 (1998).

FIGURES

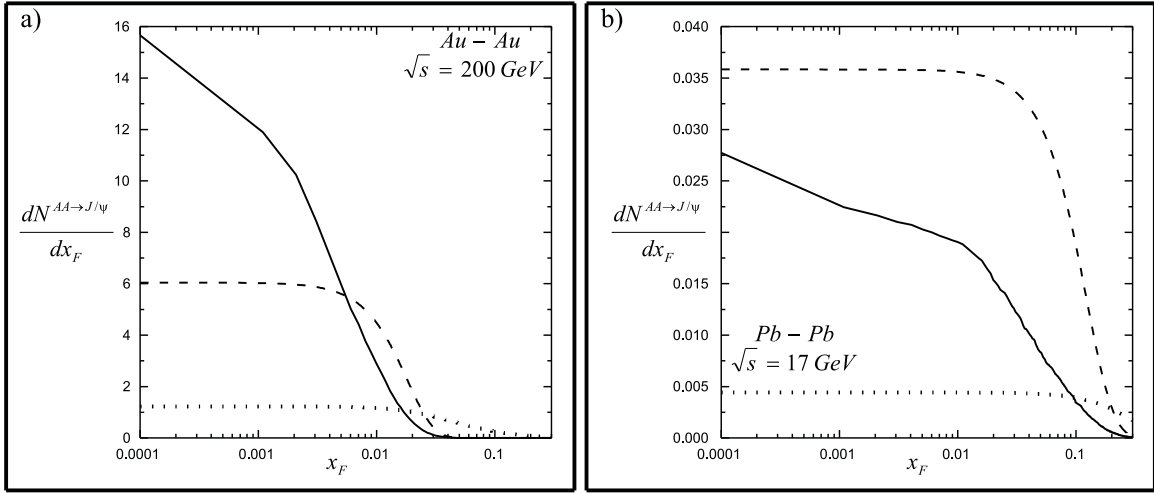


FIG. 1. Differential rate of J/ψ production

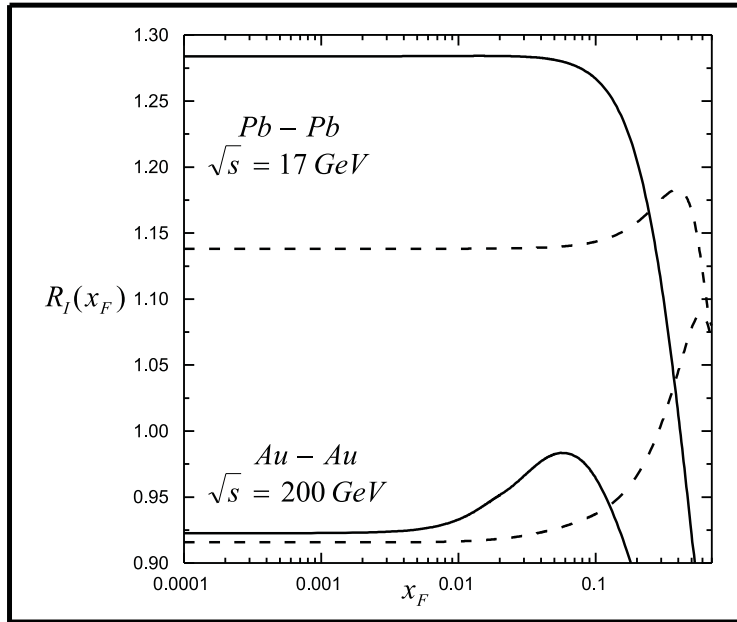


FIG. 2. Ratio $R_I(x_F)$

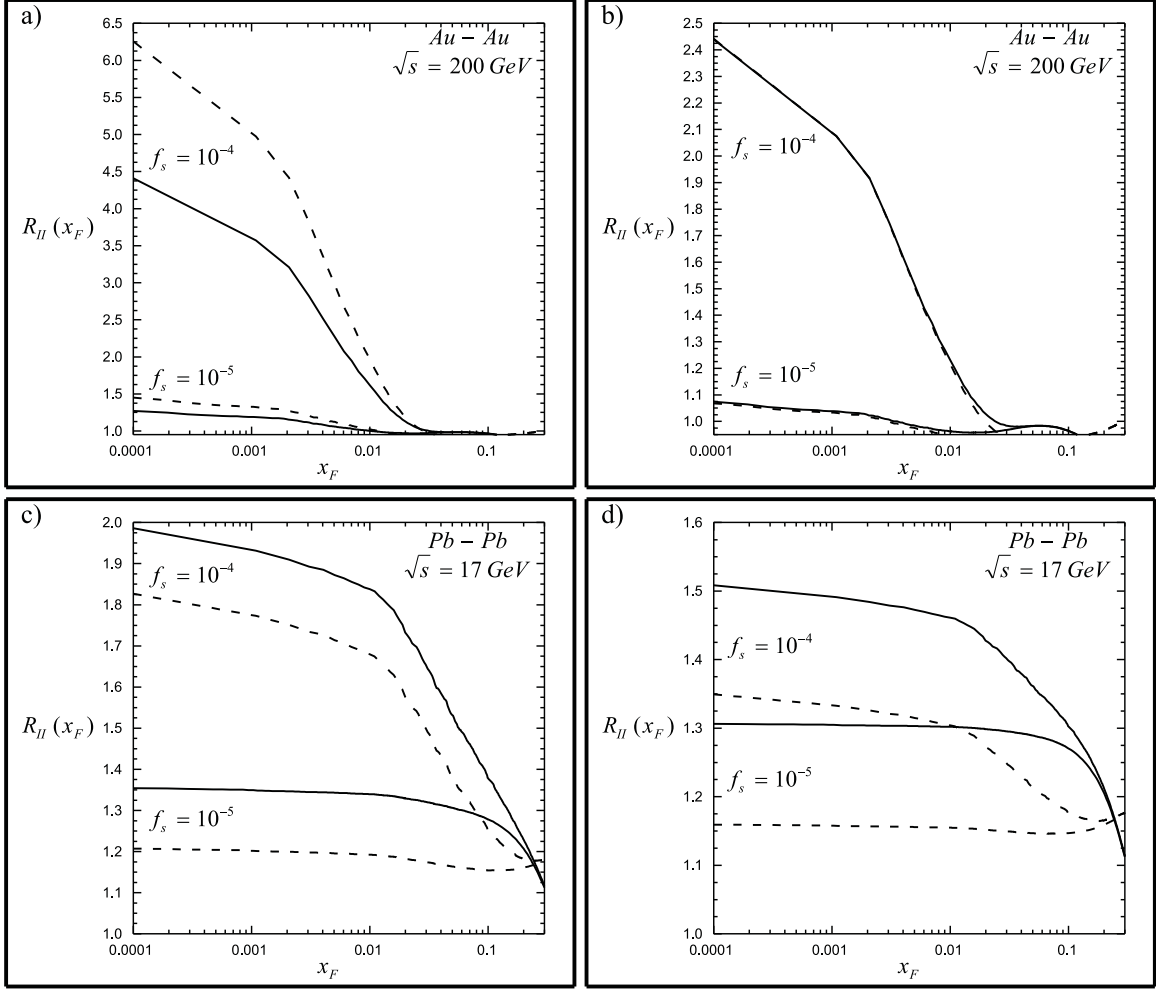


FIG. 3. Ratio $R_{II}(x_F)$

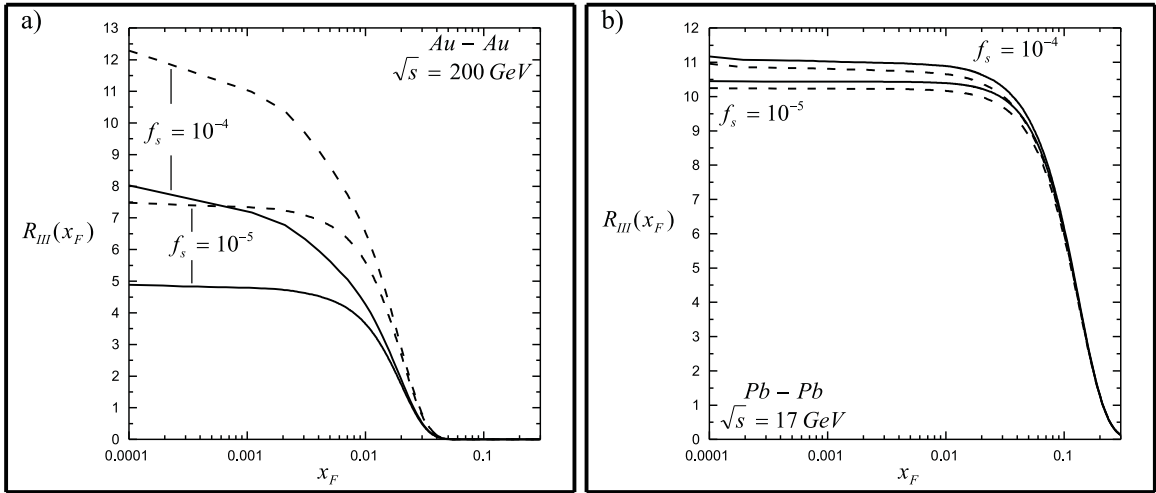


FIG. 4. Ratio $R_{III}(x_F)$

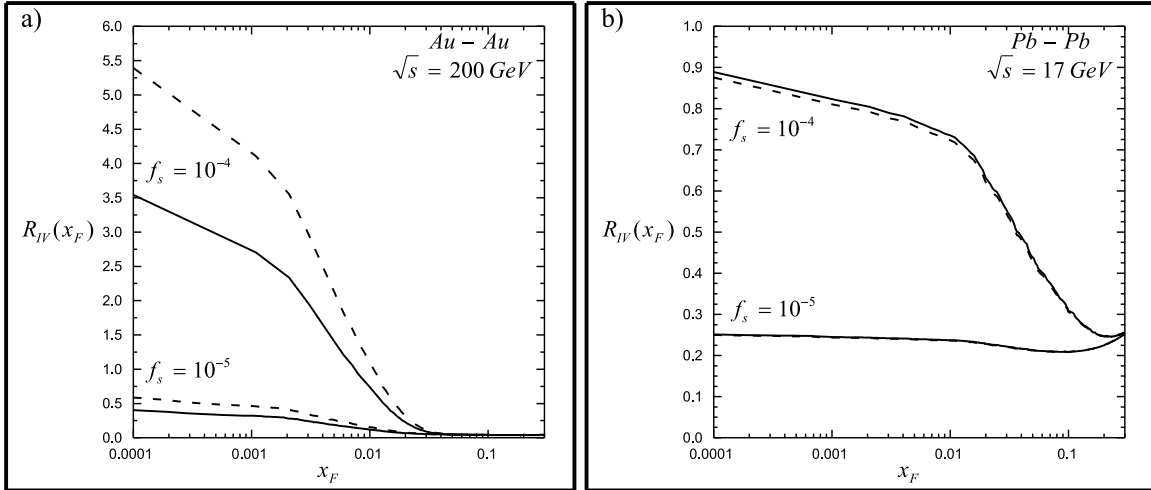


FIG. 5. Ratio $R_{IV}(x_F)$